

strip DS that does not separate into layers parallel to the basal plane (see Figs. 1 and 2). We assume that in this region of the plate there exists one EMA perpendicular to the plane of the plate. In this case one can propose the DS model shown in Fig. 6. This structure is not separated into layers parallel to the basal plane, so that the latter do not have a combined magnetic moment. An estimate of the equilibrium domain size d yields

$$d = \frac{2\hbar^4}{b_{11}-b_{12}} [2(c_{11}-c_{12})(A \cdot 2\pi M_0^2)^{1/2}]^{1/4}.$$

Thus, the proposed models describe not only the main features of the DS in an RbNiF_3 plate, but also result in a domain-size estimate close to that observed in experiment, thus indicating that these features are realistic. In addition to the two cases considered, other variants of the EMA orientation relative to the plate surface are possible, and yield similar estimates of the domain sizes. A case when the EMA is parallel to the plane of the plate is not observed in experiment.

It should be noted that in exceptional cases an analysis of the domain structures observed on plates with different orientation can reveal the sign of the constant K_3 . As a rule, however, such an analysis is made very complicated by the influence of the residual stresses on the formation of the DS.

The authors thank B. A. Ivanov for a helpful discussion of the results.

¹Institute of Physics Problems, USSR Academy of Sciences.

¹G. S. Kandaurova and Y. V. Ivanov, *Zh. Eksp. Teor. Fiz.* **70**,

666 (1976) [*Sov. Phys. JETP* **43**, 343 (1976)].

²R. V. Pisarev, I. G. Siny, and G. A. Smolensky, *Solid State Commun.* **7**, 23 (1969).

³E. I. Golovenchits, A. G. Gurevich, and V. A. Sanina, *Pis'ma Zh. Eksp. Teor. Fiz.* **3**, 408 (1966) [*JETP Lett.* **3**, 266 (1966)].

⁴A. N. Grishmanovskii, *Fiz. Tverd. Tela (Leningrad)* **16**, 2716 (1974) [*Sov. Phys. Solid State* **16**, 1755 (1975)].

⁵W. Rüdorff, I. Kändler, and D. Babel, *Z. Anorg. Allgem. Chem.* **317**, 261 (1962).

⁶M. W. Shafer, T. R. McGuire, B. E. Argyle, and G. J. Fan, *Appl. Phys. Lett.* **10**, 202 (1967).

⁷E. I. Golovenchits, V. A. Sanina, and A. G. Gurevich, *Fiz. Tverd. Tela (Leningrad)* **10**, 2956 (1968) [*Sov. Phys. Solid State* **10**, 2334 (1979)].

⁸R. D. Burbank and H. T. Evans Jr., *Acta Cryst.* **1**, 330 (1948).

⁹A. I. Belyaeva, V. V. Eremenko, V. I. Silaev, R. A. Vaishnoras, and V. A. Potakova, *Fiz. Tverd. Tela (Leningrad)* **17**, 369 (1975) [*Sov. Phys. Solid State* **17**, 233 (1975)].

¹⁰V. I. Silaev, Yu. E. Stetsenko, A. I. Belyaeva, Yu. N. Stel'makhov, and G. S. Egizaryan, *Prib. Tekh. Éksp. No. 5*, 228 (1979).

¹¹W. J. Tabor and F. S. Chen, *J. Appl. Phys.* **40**, 2760 (1969).

¹²S. V. Vonsovskii and Ya. S. Shur, *Ferromagnetizm (Ferromagnetism)*, Gostekhizdat, 1948, pp. 272 and 236.

¹³I. A. Privorotskii, *Usp. Fiz. Nauk* **108**, 34 (1972) [*Sov. Phys. Usp.* **15**, 555 (1973)].

¹⁴A. N. Grishmanovskii, V. V. Lemanov, G. A. Smolenskii, and P. P. Syrnikov, *Fiz. Tverd. Tela (Leningrad)* **14**, 2369 (1972) [*Sov. Phys. Solid State* **14**, 2050 (1973)].

¹⁵A. Hubert, *Theory of Domain Walls in Ordered Media* [Russ. transl.], Mir, 1977, pp. 47 and 74.

¹⁶J. Als-Nielsen, R. J. Birgenau, and H. I. Guggenheim, *Phys. Rev.* **B6**, 2030 (1972).

¹⁷E. M. Lifshitz, *Zh. Eksp. Teor. Fiz.* **15**, 97 (1945).

Translated by J. G. Adashko

Absorption of hypersound in stratifying solutions in the vicinity of the critical point

L. M. Sabirov, Ya. Turakulov, and T. M. Utarova

Samarkand State University

(Submitted 13 May 1980)

Zh. Eksp. Teor. Fiz. **79**, 2263–2269 (December 1980)

The scattered-light spectra were used to measure the temperature dependence of the amplitude coefficient α and the velocity v of hypersound near the critical temperature of critical-concentration solutions having an upper critical stratification point. The results of the measurement are compared with conclusions of the present-day theory. A mechanism due to the coupling between the fluctuations of the order parameter and the entropy fluctuations is considered in addition to the interaction of the acoustic mode with the diffusion mode.

PACS numbers: 43.20.Hq

1. INTRODUCTION

Second-order phase transitions near critical points are being investigated by various methods. The thermodynamic, optical, acoustic, and other properties of media in the vicinity of critical points have been the subject of many experimental and theoretical studies (see, e.g., the monographs and reviews¹⁻³). These investigations have shown that certain thermodynamic parameters and dynamic coefficients have singularities

near the critical point. In particular, the acoustic properties of a medium in the vicinity of a critical point undergoes substantial changes. A number of experimental studies^{4,5} have shown that as the critical temperature of a pure liquid and the critical stratification temperature T_c of solutions are approached, the ultrasound absorption coefficient increases noticeably. A theory of sound propagation in the critical region, with account taken of the coupling of the acoustic and diffusion modes of motion, was developed in Refs. 6

and 7-11.

A comparison of the experimental results on the absorption of ultrasound¹² with calculation by means of the formulas of the aforementioned theories shows that the character of sound propagation is satisfactorily described up to frequencies $\sim 10^8$ Hz. At the same time, at higher hypersound frequencies, the results of the experiments do not agree with the theory. Measurements of the hypersound absorption coefficient α near T_c (Ref. 13) yield much larger values than those calculated from the theoretical formulas. In subsequent studies¹⁴ it was shown that at high frequencies an important role may be assumed by the contribution made to sound absorption by a previously unaccounted-for mechanism due to the coupling between the order-parameter fluctuations and the entropy fluctuations. Thus, for solutions, an additional contribution to the absorption coefficient of hypersound is due to the irreversible equalization of the entropy between the regions with different values of the density in the sound wave.

In the present study, using the spectra of scattered light, we measured the temperature dependence of the absorption coefficient α and of the velocity v of hypersound near the critical temperature T_c in nitrobenzene-*n*-dodecane (N-D) and nitromethane-*n*-amyl alcohol (Nm-AH). For the solutions nitrobenzene-*n*-hexane (N-H) and aniline-cyclohexane (A-C), the absorption values obtained in Ref. 15 were corrected for the deviation of the exciting and instrumental functions from Lorentzians. The results of the measurements are compared with the conclusions of present-day theories.

2. MEASUREMENT PROCEDURE

The values of α and v were determined from the half-width $\delta\omega$ and the shift $\Delta\omega$ of the Mandel'shtam-Brillouin components (MBC). The experimental setup for the investigation of the Mandel'shtam-Brillouin scattering, used in the present study, is shown in Fig. 1.

The spectral instrument was a two-pass Fabry-Perot

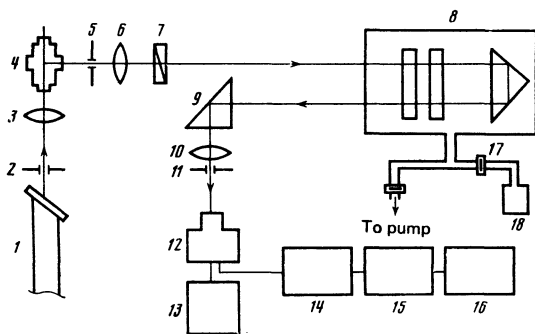


FIG. 1. Experimental setup: 1—single-frequency HeNe laser LG-159, 2—diaphragm, 3—condenser ($f = 120$ mm), 4—cell with investigated liquid, 5—diaphragm ($d = 5-8$ mm), 6—collimating objective ($f = 210$ mm), 7—polarizer (Frank-Ritter prism) 10—camera lens ($f = 270$ mm), 11—diaphragm ($d = 0.25$, mm), 12—cooled FEU-79 photomultiplier, 13—power supply for photomultiplier (VS-22), 14—emitter follower, 15—linear intensity meter PI-4-1, 16—automatic recorder (KSP-4), 17—needle leak valve, 18—flask with nitrogen.

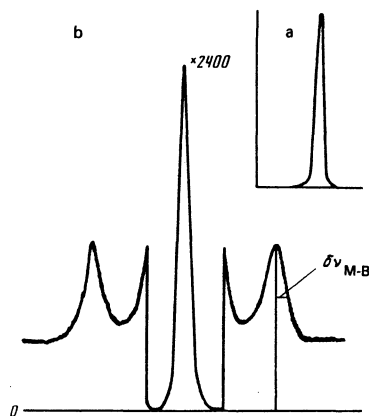


FIG. 2. Experimental spectra ($\{\Delta\nu\} = 0.417$ cm⁻¹): a—instrumental function of apparatus, b—aniline-cyclohexane solution, $\Delta t = 0.3^\circ$ C.

interferometer constructed in our laboratory, with a contrast in the spectrum $C_n \sim 4 \times 10^5$ and a sharpness (ratio of the free spectral range of the interferometer to the total instrumental half-width) $F \approx 40$. We used free spectral ranges $\{\Delta\nu\} = 0.417$ and 0.714 cm⁻¹. The spectrum was scanned by varying the gas pressure in the interferometer chamber. The scattered light was excited by a single-frequency He-Ne laser with $\lambda = 6328$ Å and ~ 2 mW power. The exciting light was polarized in a plane perpendicular to the scattering plane. The scattered light was observed at an angle $\theta = 90^\circ$ in both polarizations: in the scattering plane and perpendicular to it.

Figure 2 shows typical interference patterns of the scattered light and a plot of the instrumental function of the setup as a whole. An analysis of the shape of the instrumental function has shown that it is described by a Voigt function, and not by some other function.¹⁶ In the determination of the true half-width $\delta\omega$ of the MBC it was assumed that it has a Lorentz shape, and elimination of the instrumental function, approximated by a Voigt function, was carried out by the standard method.¹⁷

The hypersound velocity v and its amplitude absorption coefficient α were determined from the relations

$$v = \frac{c\Delta\nu}{2n\nu_0 \sin(\theta/2)}, \quad (1)$$

$$\alpha = 2\pi c\delta\nu/v. \quad (2)$$

Here c and ν_0 are the velocity and frequency of the exciting light, n is the refractive index of the solution, $\Delta\nu = \delta\omega/2\pi$ and $\delta\nu = \delta\omega/2\pi$.

We have obtained for the investigated solutions the coexistence curves and determined the critical parameters gathered in Table I.

TABLE I.

Solution	c_c , molar fractions	T_c , °C	Solution	c_c , molar fractions	T_c , °C
N-H	0.6 <i>n</i> -hexane	20	N-D	0.43 <i>n</i> -dodecane	28.2
A-C	0.56 cyclohexane	32.2	Nm-AH	0.39 <i>n</i> -amyl alcohol	24.5

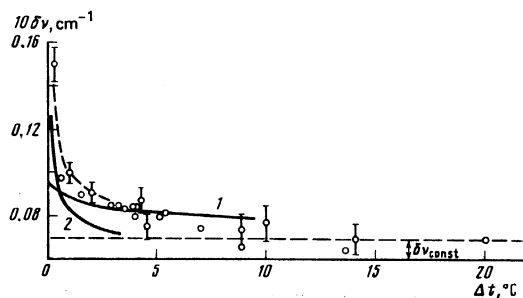


FIG. 3. Dependence of MBC half-width on $\Delta t = (t - t_c)$ in nitrobenzene-n-hexane mixture: points—experiments; curve 1—calculation by formula (4); 2—calculation by formula (3'); dashed—sum of curves 1 and 2.

3. MEASUREMENT RESULTS AND THEIR DISCUSSION

The measured half-widths $\delta\nu$ of the MBC for the four solutions investigated by us, as functions of their approach $\Delta t = t - t_c$ to the critical temperature are shown in Figs. 3-6. As follows from the figures, when the critical temperature is approached the MBC half-width is at first practically independent of Δt , and near t_c ($\Delta t \sim 1-1.5^\circ$) it increases strongly. In Table II are given the temperature intervals in which the growth of $\delta\nu$ is observed, as well as the sound absorption amplitude coefficient calculated from $\delta\nu$ for all the investigated solutions.

It follows from Table II that in the indicated temperature interval the first three solutions are characterized by an increase of $\delta\nu$, and consequently of α , from 60 to 210%, and only in Nm-AH does α increase by only 20%.

According to the coupled-mode theory⁶⁻⁸ the temperature dependence of the half-width $\delta\nu$ or of α can be obtained from the following relations:

$$\alpha = c\delta\nu_D/v = Af^d I(d); \quad (3)$$

Since the singularity of the sound velocity v as $t \rightarrow t_c$ is small, it can be assumed that⁶

$$\delta\nu_D \sim Af^d I(d), \quad (3')$$

where $d = cf^{-1/2} \Delta t$, f is the frequency of the sound, and $I(d)$ is an integral numerically calculated by Fixman⁶

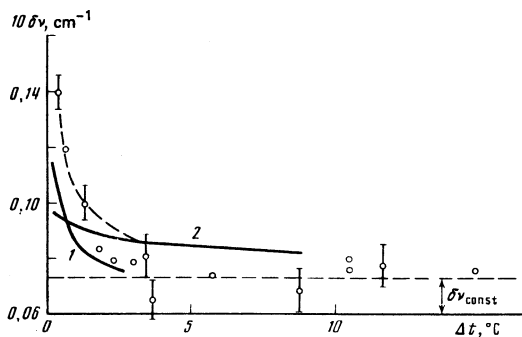


FIG. 4. Dependence of MBC half-width on $\Delta t = (t - t_c)$ in the nitrobenzene-n-dodecane mixture: points—experiment; curve 1—calculation by formula (3'); 2—calculation by formula (4); dashed—sum of curves 1 and 2.

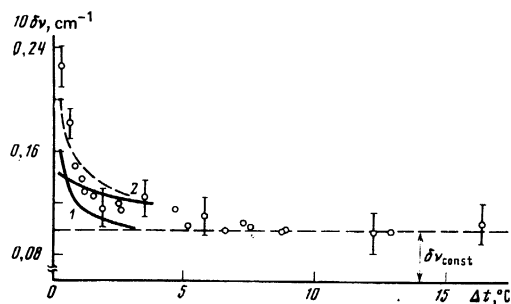


FIG. 5. Dependence of MBC half-width on $\Delta t = (t - t_c)$ in aniline-cyclohexane mixture: points—experiment; curve 1—calculation by formula (3'), 2—calculation by formula (4'); dashed—sum of curves 1 and 2.

(we use here the relevant data). The subscript D of $\delta\nu$ corresponds here to the excess absorption due to the interaction of the acoustic and diffusion modes. The parameters A and C should depend weakly on the temperature and are assumed usually constant in the calculations.

Expression (3') yields the so-called excess absorption or excess half-width, the latter defined as the result of subtracting from the total MBC half-width that part $\delta\nu_{\text{const}}$ which does not depend or depends little on the temperature and is determined by the value of $\delta\nu$ far from t_c . The calculation of the excess value $\delta\nu_D$ by formula (3') was carried out at the values of the parameters A and C listed in Table II.

The results of the calculation of $\delta\nu_D$ are represented by curves 1 of Figs. 3-5. As seen from these figures, in the solutions N-H, A-C, and N-D the calculated values of ν_D are less than those measured in experiment. But in the solution Nm-AH the result of the experiment are quite satisfactorily described by expression (3).

It should be noted that for the solutions N-H and N-D the values of A and C are the same and equal to the values used in Ref. 13 for the N-H mixture. In general, the value of A was chosen such as to satisfy the equality $\delta\nu_D = \delta\nu - \delta\nu_{\text{const}}$ at not too small values Δt , for which $I(d)$ is minimal. The value of C is the same for all solutions.

Adzhemyan *et al.*¹⁴ have taken into account the fact that at high frequencies the interaction of the entropy and concentration fluctuations can make a substantial contribution to the sound-absorption coefficient. The characteristic frequency of the process, $\omega_\chi = \chi/r_c^2$ (χ is the thermal diffusivity coefficient and r_c is the cor-

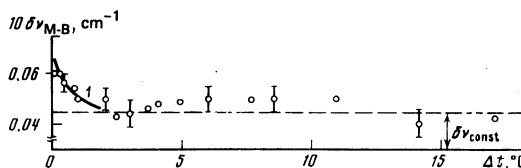


FIG. 6. Dependence of MBC half-width on $t = (t - t_c)$ in nitromethane-n-amyl alcohol mixture; points—experiment, 1—calculation by formula (3').

TABLE II.

Solution	$\Delta t, ^\circ\text{C}$	$10^6\nu, \text{cm}^{-1}$	$\nu, \text{m/sec}$	α, cm^{-1}	$A, \text{sec}^{-0.25}$	$C, \text{sec}^{-0.5}, \text{deg}^{-1}$	$\chi_{\text{I}}/\chi_{\text{II}}$
I - II							
N - D	3	0.08	1290	11680	31	$9 \cdot 10^4$	1.1
	0.4	0.14	1320	20000			
N - H	4	0.08	1240	13000	31	»	0.64
	0.2	0.15	1280	22000			
A - C	6	0.1	1315	15000	46.8	»	1.1
	0.3	0.22	1342	32000			
Nm - AH	2	0.045	1245	7560	19	»	1
	0.1	0.060	1264	8940			

relation radius) is much higher than the characteristic frequency of the diffusion process $\omega_d = D/r_c^2$ (D is the diffusion coefficient).

According to the formulas of the theory of Ref. 14, which take into account the contribution made to the MBC half-width by the interaction of the entropy and density fluctuations,

$$\delta\nu_s = \frac{2\pi^2 f r_c T \rho^2 c_p v^2 B (\partial\chi/\partial c)_{p,T}}{\chi} \varphi(\omega). \quad (4)$$

We have introduced here the notation

$$\varphi(\omega) = \left(1 + \frac{\tilde{\omega}^{\eta_1}}{2^{\eta_1}} - \frac{\tilde{\omega}^{\eta_2}}{2^{\eta_2}}\right) / \left(1 + \tilde{\omega}^2\right),$$

$\tilde{\omega} = \omega/\omega_\chi$, ρ is the density, T is the temperature, and c_p is the specific heat at constant pressure. We used in the calculation the typical value $\chi = 10^{-3} \text{ cm}^2/\text{sec}$, indicated in Ref. 14, for stratifying mixtures, and $B = 5 \times 10^{-8} \text{ cm}$ (B is the coefficient in the Ornstein-Zernike approximation³). The correlation radius r_c was calculated from the formula $r_c = r_0 \varepsilon^{-0.63}$, where $\varepsilon = \Delta t/T$, and r_0 was taken from Anisimov's paper.³

For the N-H mixture we used the temperature dependence given for c_p in Ref. 18. In the mixtures A-C and N-D, owing to the lack of data on c_p , we used the same values as for N-H. The velocity ν was determined from the shift of the MBC in the same experiments. For the N-D and Nm-AH solutions, the temperature dependence of ν is shown in Figs. 7 and 8, while for the solutions N-H and A-C they are given in Ref. 15.

The value of $(\partial\chi/\partial c)_{p,T}$ for stratifying mixtures was estimated in Ref. 14, where it was found that the most typical value of the derivative of the thermal-diffusivity coefficient with respect to concentration is $3 \times 10^{-11} \text{ cm}^3/\text{erg}$. In calculations by formula (4) we used this value for the mixtures N-H, N-D, and A-C.

Curves 2 for $\delta\nu_s$ in Figs. 3-5 were calculated by

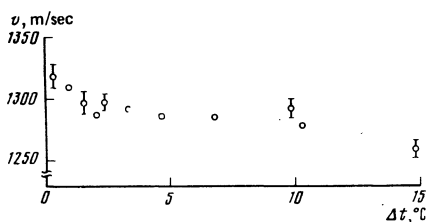


FIG. 7. Dependence of hypersound velocity ν on Δt in nitrobenzene-n-dodecane mixture.

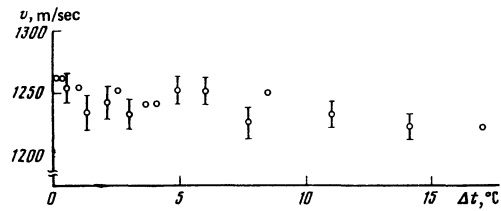


FIG. 8. Dependence of hypersound velocity ν on Δt in nitromethane-n-amyl alcohol mixture.

formula (4). The dashed curves in Figs. 3-5 are the sums of curves 1 and 2, i.e., the sums of the contributions of the two mechanisms considered above to the sound absorption. It follows from the results that the temperature dependence of $\delta\nu$ agrees with the calculation in the solutions N-H, N-D, and A-C, if $\delta\nu$ is taken to be the sum of the values calculated from (3') and (4). The fact that the interaction of the concentration and entropy fluctuations make no contribution to the excess half-width of the MBC in the Nm-AH mixture can be attributed to the fact that the factor $(\partial\chi/\partial c)$ is close to zero.

The last column of Table II gives the ratios of the coefficients of the thermal diffusivity of the I-st and II-nd components of the solutions. The values of χ were calculated by us for the pure components of the solutions at $t = 0^\circ\text{C}$ and at normal atmospheric pressure, using a semi-empirical formula for the thermal conductivity, taken by us from Ref. 19. As seen from Table II, in the Nm-AH solution the ratio $\chi_{\text{I}}/\chi_{\text{II}} = 1$, in other words, the value of χ in pure nitromethane and in pure n-amyl alcohol are equal, whereas in the solutions N-H, N-D, and A-C the thermal diffusivities of the pure components differ from one another. The identical values of χ in the pure components of the solution cause the derivative of the thermal diffusivity with respect to concentration to be zero, and with it $\delta\nu_s = 0$.

Thus, in the solution Nm-AH the excess absorption can be attributed to the interaction of the sound and diffusion modes. In the solutions N-H, N-D, and A-C, however, an additional contribution to the excess hypersound absorption as $\Delta t \rightarrow 0$ is made by the interaction of the concentration and entropy fluctuations.

We take the opportunity to thank I. L. Fabelinskii, S. V. Krivokhizha, and A. A. Sobyenin for helpful discussions of the results, as well as A. K. Atakhodzhaev for constant interest in the work.

¹I. L. Fabelinskii, *Molecular Scattering of Light*, Plenum, 1968.

²*Physical Acoustic*, Vol. 6, R. Thurston, ed. Academic, 1970.

³M. A. Anisimov, *Usp. Fiz. Nauk* **114**, 249 (1974) [*Sov. Phys. Usp.* **17**, 722 (1975)].

⁴G. D. Arrigo, L. Mistura, D. Sette, and J. L. Hunter, *The Goth Intern. Congr. Acoustics*, Tokyo, 1968, Vol. 5, Unesco (Paris), 1969, j-89.

⁵P. Taraglia, G. D. Arrigo, L. Mistura, and D. Sette, *Phys. Rev. A6*, 1627 (1972).

⁶M. Fixman, *J. Chem. Phys.* **36**, 1961 (1963).

⁷K. Kawasaki and M. Tanaka, *Proc. Phys. Soc.* **569**, 791 (1967) [sic!].

- ⁸K. Kawasaki, *Phys. Rev. A* **1**, 1750 (1970).
⁹L. P. Kadanoff and J. Switt, *Phys. Rev.* **166**, 89 (1968).
¹⁰V. P. Romanov and V. A. Solov'ev, *Akustich. zh.* **11**, 84, (1965); **14**, 262 (1968) [*Sov. Phys. Acoust.* **11**, 68 (1965); **14**, 224 (1968)].
¹¹L. A. Chaban, *ibid.* **21**, 104, 286 (1975) [**21**, 64, 177 (1975)].
¹²L. Mistura, *Rend. Scu. int. fiz. Enrico Fermi Varenna sul Lago di como*, 172, Corso 1971, p. 563.
¹³S. H. Chen and N. Polonsky, *Phys. Rev. Lett.* **20**, 909 (1968).
¹⁴L. V. Adzhemayn, L. I. Adzhemyan, V. P. Romanov, and V. A. Solov'ev, *Akustich. Zh.* **23**, 840 (1977) [*Sov. Phys. Acoust.* **23**, 482 (1977)].
¹⁵S. V. Krivokhizha, Ya. Turakulov, and L. Sabirov, *Zh. Eksp. Teor. Fiz.* **78**, 1579 (1980) [*Sov. Phys. JETP* **51**, 793 (1980)].
¹⁶S. M. Lindsay, S. Burgess, and L. W. Shepherd, *Appl. Optics* **16**, 1404 (1977).
¹⁷H. C. Hulst and J. J. Reesink, *Astrophys. J.* **106**, 121 (1947).
¹⁸V. K. Semenchenko and V. P. Smirnov, *Zh. Fiz. Khim.* **25**, 362 (1951).
¹⁹Tablitsy fizicheskikh velichin. Spravochnik (Tables of Physical Quantities, Handbook), Atomizdat, 1976.

Translated by J. G. Adashko

The macroscopic description of the effective field in certain dielectrics

Yu. S. Barash

Institute of Terrestrial Magnetism, the Ionosphere, and Radio Wave Propagation, Academy of Sciences of the USSR, Leningrad Section

(Submitted 20 May 1980; resubmitted 11 July 1980)

Zh. Eksp. Teor. Fiz. **79**, 2271-2281 (December 1980)

Macroscopic formulas which essentially generalize the Lorentz-Lorenz relation are found for the effective field and its first derivatives. It can be seen from the derived equations that the quantity g is in general not equal to $4\pi/3$, but is related to the dielectric constant and its derivatives with respect to density and shear deformations. The proposed derivation uses results of the macroscopic theory for the volume density of electric forces in dielectrics.

PACS numbers: 77.90. + k

1. INTRODUCTION

The effective field \mathbf{E}_{eff} acting on a certain particle in a condensed medium is the average of the microscopic field under the condition that the given particle is in a definite state. On the other hand the macroscopic field \mathbf{E} that appears in Maxwell's equations is obtained from the microscopic field by averaging over the states of all the particles. Consequently, when the correlations between the particles in their motion or spatial distribution are taken into account the effective field \mathbf{E}_{eff} and the macroscopic field \mathbf{E} are not equal. This difference leads to the so-called local-field effects in condensed media, which are well known and have been studied for crystals^{1,2} and also for liquids³ and plasmas.^{4,5}

The macroscopic description of effective fields is by no means always possible. This is clear already from the fact that the field \mathbf{E}_{eff} is in general a function of the state of the particle and is thus basically a microscopic quantity. The difference between the fields acting on different particles is often important. It is well known, for example, that the Davydov splitting in molecular crystals with several molecules in the elementary cell is due to the differences between the fields acting on these molecules; even in isotropic cubic crystals with several molecules in an elementary cell the fields acting on these molecules differ considerably.¹ There are also differences between the fields acting on different components in many-component liquids, and similar differences in a number of other cases. Other cases are also encountered in which with reasonable accuracy

one can neglect the differences between the effective fields acting on the various particles, and thus it makes sense to consider a single average effective field for all particles. This applies, for example, to cubic crystals with one molecule in the elementary cell, to some one-component simple liquids, and also, under certain circumstances, to plasmas. It is clear from the start that in a macroscopic approach, with the properties of the medium described with one dielectric constant, we have the only sort of case in which a description in terms of effective fields may be possible. If this condition holds, together with certain definite supplementary assumptions, it is well known that the effective field is connected with the macroscopic field by the Lorentz-Lorenz formula

$$\mathbf{E}_{\text{eff}} = \mathbf{E} + \frac{4\pi}{3} \mathbf{P} = \frac{\epsilon + 2}{3} \mathbf{E}. \quad (1)$$

This formula is an approximate one, and only in cases for which its use is justified (cubic crystals,² nonpolar liquids³) it usually provides only a qualitative account of the difference between the effective and the macroscopic fields.

In many cases, however, the Lorentz-Lorenz formula is incorrect even in a qualitative description of the effective field. The best known example of this is a plasma with the dielectric constant

$$\epsilon = 1 - 4\pi e^2 N / m\omega^2,$$

for which, as is clear from the microscopic theory, the